An evaporation source for ion beam assisted deposition in ultrahigh vacuum

J. Kirschner,[a] H. Engelhard, and D. Hartung
Max-Planck-Institut für Mikrostrukturphysik Weinberg 2, 06120 Halle, Germany

(Received 16 October 2001; accepted 7 August 2002)

We describe the design, construction, and operation of an ion beam assisted deposition source for molecular beam epitaxy in ultrahigh vacuum. At a typical deposition rate of a monolayer per minute, the source may be operated in each of five modes: using self-ions from the vapor, self-ion plus noble gas ions from an additional gas inlet, both pulsed or continuous, or with complete suppression of ions. The source is based on electron bombardment heating of a metal rod or a crucible while the ions generated from the vapor are focused electrostatically onto the sample. Additional ions may be extracted from a noble gas stream injected into the ionization region. Examples for each of the different modes are given for Co deposition onto Cu(111), a system known to resist layer-by-layer growth. © *2002 American Institute of Physics.* [DOI: 10.1063/1.1511791]

I. INTRODUCTION

In many technical thin film deposition processes ion beam assisted deposition (IBAD) is known to have beneficial effects on the properties of the films. For reviews see Ref. 1–6. In most of these applications the fast generation of coatings, optical layers, etc., with thickness in the range of microns is at the center of interest. By contrast, when growing epitaxial films in the range of atomic monolayers the layer-by-layer growth mode is most often desired in order to produce films of optimum smoothness. Though there are many examples of natural layer-by-layer growth (most often when the surface energy of the overlayer is much smaller than that of the substrate) this growth mode is rather the exception than the rule (even for homoepitaxy). Therefore, several schemes have been invented in the past to stimulate layer-by-layer growth in cases where it does not occur naturally. Essentially two alternative approaches have been used.

(i) Reducing the so-called Ehrlich–Schwoebel barrier at the circumference of a growing island which tends to hinder atoms landed on top of the island to reach the terrace below. This can be done by introducing so-called ''surfactants,'' i.e., atomic or molecular species which aggregate at or near island edges and which reduce the barrier height without being incorporated themselves into the growing film. Thus, surfactants play a similar role as catalysts in chemical reactions.[6–12]

(ii) Layer-by-layer growth may also be favored by increasing the number density of new islands at the beginning of the first monolayer of the film and of each subsequent layer.[13] The statistical probability at a given coverage of two randomly arriving atoms to land on the same island to from a nucleus for the next layer is lower for many small islands than for a few large ones. Additionally, interlayer mass transport on small islands is enhanced since the attempt frequency to overcome the step edge barrier is higher because the travel distance from the center of the island to its edge is smaller. The surface diffusion on top of a small island is also predicted to be faster than on a large island[14] and the barrier height itself may decrease with decreasing island size.[15]

In the present context the approach of improving layer-by-layer growth by increasing the island density is of prime interest. The island density may be enhanced by statistical means or by creating a sufficient number of nucleation sites. In pulsed laser deposition[16–18] the instantaneous flux after a laser pulse is very high [about 5–6 orders of magnitude higher than in ordinary molecular beam epitaxy (MBE)] which leads to a high instantaneous adatom density and consequently to short diffusion paths among neighboring atoms having arrived at the same time on the substrate. This in turn leads to a strongly enhanced nucleation rate and high island density. The alternative way of creating nucleation centers has been recently discussed in the literature,[19–22] namely the creation of defects by kinetic ion bombardment during deposition. It has been shown that the adatoms created by a single ion impact may serve as efficient nucleation centers,[23] while the voids are filled rapidly. The ion bombardment may be applied continuously with significant improvement of the layer-by-layer growth, either by ions from the vapor itself or by ions from a separate noble gas ion gun.[24] It has been suggested by Refs. 20–22 that a short but intense noble gas ion beam pulse at or near the beginning of a new layer may improve layer-by-layer growth even more. This has been proven by observation of the intensity oscillations in coherently diffracted He beams[22] and directly by scanning tunneling microscopy.[24]

In this article we describe the design and operation of an evaporation source for molecular beam epitaxy applications of metals with optional ion beam capabilities. The source is designed for ultrahigh vacuum (UHV) applications at low to moderate deposition rate [of order atomic monolayer(s) per minute] under clean conditions. The source may be operated in five different modes:

(i) vapor deposition only with suppression of ions;

[a]Electronic mail: sekrki@mpi-halle.mpg.de

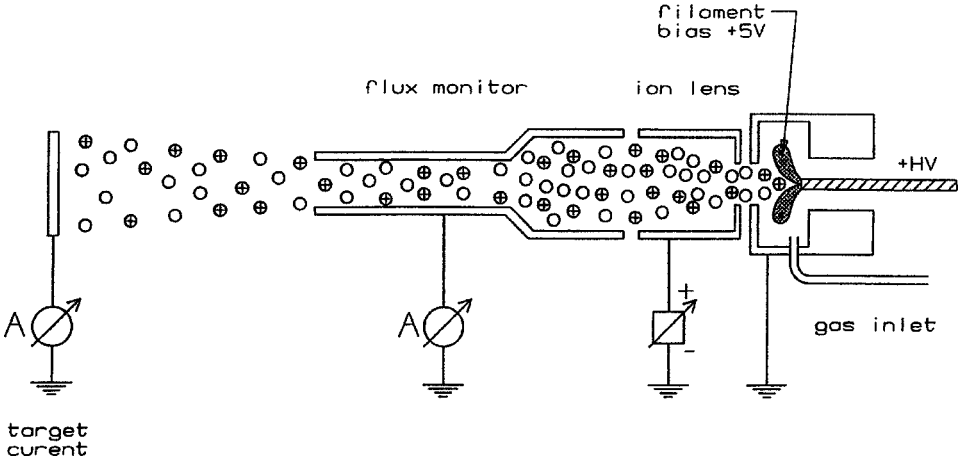

FIG. 1. Principle of operation of the source for IBAD–MBE. The evaporation rod is heated by electrons from a circular wire loop. The electrons ionize a fraction of the vapor surrounding the tip of the evaporation rod. The ions are extracted through the opening in the housing and may be partially collected on the flux electrode. Alternatively, they may be focused by the lens electrode onto the target. An additional gas inlet serves to direct a stream of noble gas atoms towards the evaporation region where they are likewise ionized and focused onto the target. Under the operating conditions of Table III an ion fraction of more than 10% was obtained.

(ii) pulsed or continuous addition of self-ions from the vapor; and
(iii) pulsed or continuous addition of noble gas ions and self-ions to the vapor beam.

In typical ion beam assisted deposition systems, the deposition source and the ion beam are completely independent. This allows the two processes to be controlled independently and to set the parameters with great flexibility. In our case the two processes are partly coupled since the ion generation occurs simultaneously with the evaporation. While the ions can be turned off completely, their maximum flux cannot be increased arbitrarily, as is discussed later. On the other hand, our design is purposely intended to deposit ultrathin films in the monolayer range. It is mounted on a single 35 mm CF flange, occupies minimal space around the sample, and is easily mounted to any existing ultrahigh vacuum chamber. Therefore, it is ideally suited in cases where the space requirements, cost, and complexity of a typical IBAD system are inadequate for the purpose of studying monolayer films on single crystals in UHV.

II. PRINCIPLE OF OPERATION

The present IBAD–MBE source is based on the design principles developed by one of the authors (J.K.) about a decade ago.[25] Similar designs have been described by Jones *et al.*[26] and Jonker.[27] It is characterized by a metallic rod (or crucible) heated by a concentric thermal electron flux from a W filament, with a typical voltage of 500–1500 V between rod and filament (see Fig. 1). During evaporation a certain atom density around the rod is established, with an estimated equivalent pressure in the 10^{-8} mbar range. A few of these gas atoms are ionized by the electrons and accelerated towards the wall of the housing. When passing the aperture, they travel on straight lines until some of them are intercepted by the collector electrode or, eventually, by the target. Since for a given material, geometry, accelerating voltage, and constant emission current, the ratio between the ionized metal atoms arriving at the collector electrode and the neutral metal atoms arriving at the target is a constant, the source may be calibrated against a quartz thin film monitor or, e.g., reflection high-energy electron diffraction oscillations. The reproducibility can be better than 5% when carefully maintaining the parameters.

The idea underlying the present design of the IBAD–MBE source is to utilize the ion flux generated from the vapor or additional rare gas atoms as an additional source of kinetic ions to assist the growth of the film. While the kinetic energy distribution of the ions is of no importance for the operation of the flux monitor, any ion optical manipulation requires at least the knowledge of the ion energy distribution. We measured this distribution by means of a dispersive analyzer with a deceleratering input lens in the constant pass energy mode (100 eV), located about 15 cm from the end of the source. Some results are shown in Fig. 2 with Co, at an emission current of 8 mA for +700, +800, and +900 V at the rod. The distributions are asymmetric, with a peak at the energy corresponding to the rod voltage, with a long tail towards lower energies. The high-energy cutoff coincides with the rod voltage within the uncertainty of the energy calibration of the spectrometer of 0.3%. The shape of the

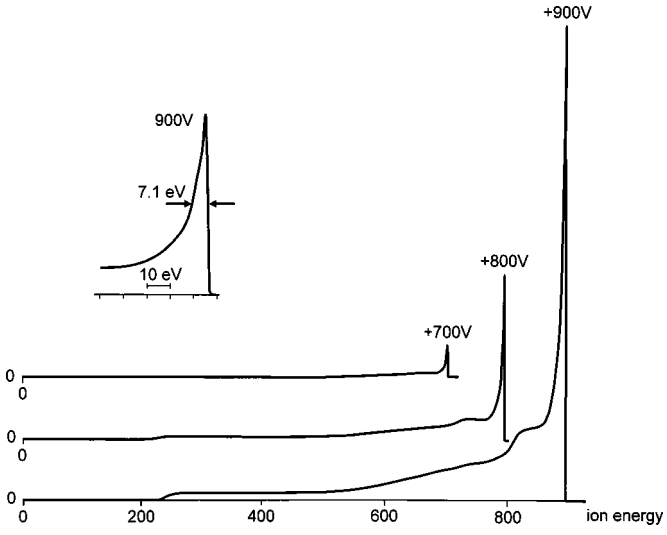

FIG. 2. Energy distribution curves of positive ions leaving the source for three different potentials at the Co rod at constant emission current of 8 mA. The inset shows the peak region on an enlarged scale. The remarkably sharp distribution is asymmetric, with a sharp high-voltage cutoff at the energy corresponding to the rod voltage.

distributions is essentially independent of the rod voltage. The peak values drop strongly with decreasing rod potential because the evaporation rate drops steeply with the heating power. If the measurements are done with variable emission current, such that the heating power is kept constant, the peak values are nearly the same. The inset shows the peak region on an enlarged scale. (at 900 V, 8 mA), with a measured full width at half maximum of 7.1 eV. Taking the energy resolution of the spectrometer into account ($\sim$3 eV), this yields a remarkably narrow energy width of about 6.5 eV. These findings may be understood in the following way: (see Fig. 1): the highest ionization probability is at the region of highest electron density. This is around the tip of the metal rod and a few millimeters in front of it. The potential drop from the rod to the housing is largest just in front of the rod and smaller afterwards. The highest ionization probability is therefore just in front of the tip at a potential close to that of the rod. This explains the asymmetric ion energy distribution with a sharp cutoff at maximum energy. The energy distribution was found to be independent of the electron emission current. Since we thus deal with a rather sharp ion energy distribution, simple electrostratic lenses may suffice to focus the ions onto the target. This is accomplished by the decelerating Einzel lens at 75%–80% of the rod potential. It projects a magnified image of the ionization region onto the target. At a target distance of 51 mm the ion beam diameter is about 5 mm. In critical situations it is advisable to scan the ion beam profile at the target position since a displacement of the rod from the geometrical axis, either by the original mounting or by a thermal drift during operation, may shift the ion beam away from the optical axis, in proportion to the lateral magnification.

By means of the focusing lens the ratio of ions to neutrals at the target may be changed strongly. For a typical geometry (see Sec. V) the target current varies by more than one order of magnitude from the lens at ground potential to the lens set at the focusing condition. This ratio is also affected by the working distance between the front end of the source and the target: it increases somewhat with increasing distance since the neutral flux falls quadratically with the distance from the rod end while the lens magnification increases less strongly. However, for typical geometries this effect may in practice not enhance the ion-to-neutral ratio by more than 50%. One will also not increase the working distance too much because the deposition rate decreases strongly.

The ion-to-neutral ratio is also strongly affected by the operation of the evaporation source. The emission current enters twofold into the ion flux: first, the heating power is directly proportional to the electron current. Second, the ionization probability is also directly proportional to the electron current. Therefore, if one wishes to have a high ion-to-neutral ratio one operates the source at high emission current (limited by space charge) and low rod voltage such as to achieve just sufficient heating power to have an adequate evaporation rate from the rod. In our case this is limited to about 20 mA emission current, not sacrificing too much of the filament lifetime. On the other hand, one should not go to extremely low voltages since the kinetic effects due to the ions at the target (most importantly creation of adatoms as nucleation centers) decrease strongly at low energy. As a good compromise 14 mA at 600 V for Co deposition as an example has been found. This may yield an ion-to-neutral ratio of 6% at the target. As noted in Ref. 24, a concentration of 10% of Ar^+ at 400 eV improves the growth of Pt on Pt(111) substantially in this context.

If a pulsed ion beam is desired, this may be easily done by switching periodically the lens potential to ground. The remaining ion flux is negligible.

For cases where a strong ion beam in pulsed operation is necessary, our design incorporates an additional gas inlet. A capillary is connected to a leak valve at the source flange. We only used noble gases (Xe or Ar). By this means one may locally create a higher gas density in front of the evaporation rod, which may enhance the ion flux by one order of magnitude relative to the operation without gas inlet. The use of reactive gases has not yet been tested.

The absolute current is limited by the ionization region shifting away from the rod (and with it the peak of the ion energy distribution) when the gas density becomes so high that the electrons ionize gas atoms with significant probability before they reach the vicinity of the rod. If the IBAD–MBE source is operated essentially as an ion source, the total ion flux is thus limited to about 1 μA. If higher ion fluxes are needed, one should use a conventional ion gun, preferably a differentially pumped one.

A further variant of the gas inlet has also been tried: direct gas admission by a central metal capillary, serving simultaneously as the evaporation material supply. Replacing the evaporation rod by a capillary of the material to be evaporated is a simple solution in those cases where capillaries of the desired materials can be made. However, for the sake of general use of our source we designed it with a lateral gas inlet (see Fig. 3), not precluding a central capillary inlet via the central high voltage (HV) flange. Since in this case an isolating tube has to be inserted somewhere between the leak valve at ground potential and the capillary end at high voltage, one has to take care to prevent spontaneous gas discharges somewhere along this path.

III. DESCRIPTION OF THE SOURCE

The mechanical design of our source is shown in Fig. 3 (slightly simplified). The evaporator and ion optics are mounted on a multiport adapter[28] with one CF35 and four CF16 flanges. The housing of the evaporator is supported by a stainless steel water pipe (with a concentric inlet pipe), welded into an extra bore in the adapter. The housing is made of an oxygen-free high-conductivity copper cylinder (wall thickness 13 mm). The length of this cylinder is longer than required by mechanical requirements to provide for a large thermal mass and for an efficient heat transfer to the water cooling pipe soldered along its length. An optional thermocouple, connected to the electrical feedthrough,[29] may serve to control its temperature. The cooling water is pumped by a small aquarium pump,[30] immersed into a 10 l water reservoir. During typical operation, also over extended periods of time, the temperature of the Cu cylinder hardly reaches

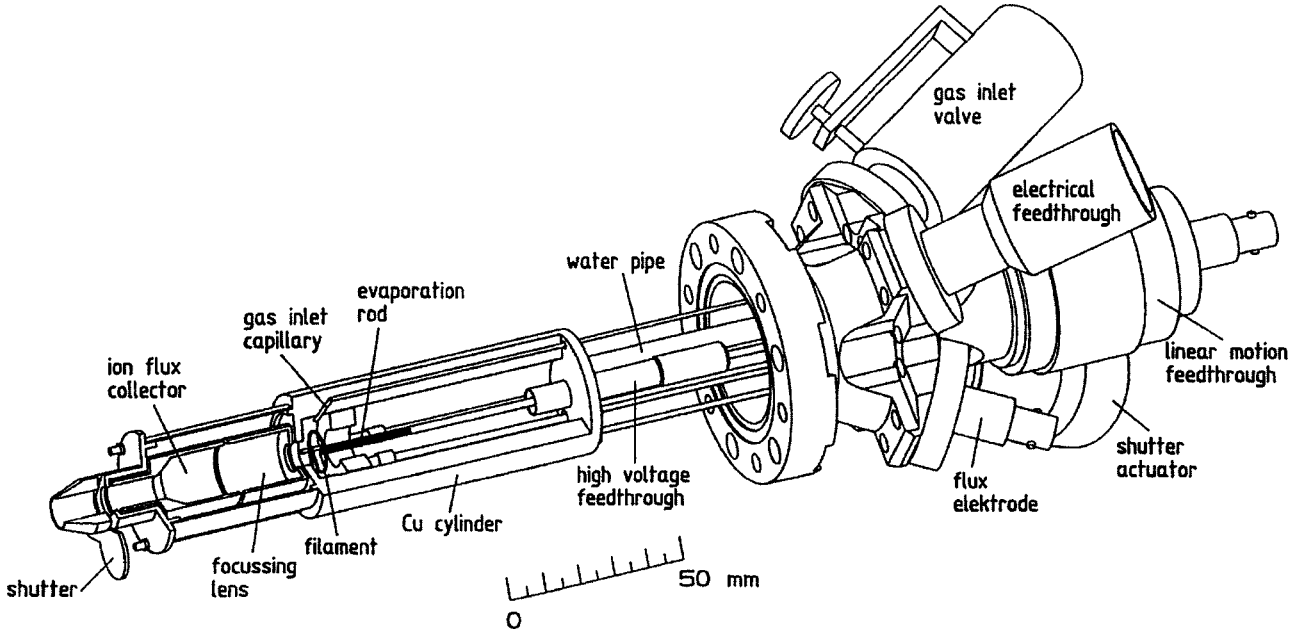

FIG. 3. Drawing of the IBAD–MBE source. Only nonmagnetic materials and parts have been used.

45 °C, while the temperature rise of the water reservoir remains negligible. Without cooling the temperature of the cylinder rises to 120–150 °C (with the HV to the evaporation rod turned off). This feature may be used as a moderate internal bakeout of the source structure. The center sleeve of a high voltage feedthrough passes through a bore in the bottom plate of the cylinder, also made of Cu. This serves to center the evaporation rod, spot welded to the central pin of the feedthrough, onto the cylinder axis. The central pin is connected to an electrical MHV feedthrough, sitting on a linear displacement feedthrough[31] of 25 mm travel. In this way the shortening of the evaporation rod, due to its evaporation, may be compensated. The overall length of the coupling rod (~150 mm) is sufficient to effectively isolate the heat generated at the tip of the evaporation rod from the electrical feedthrough. Below the top plate sits a circular tungsten filament (diameter 0.125 mm, active length 37 mm) held in a place by two low voltage feedthroughs mounted in a ring. A gas capillary (1.5 mm outer diam, 0.2 mm wall thickness) goes through a small bore through the Cu cylinder and aims at the tip of the evaporator rod. It is connected to a gas inlet valve[32] via a double-sided CF16 flange. The cylindrical focusing lens and the ion flux collector are mounted on top of the Cu cylinder as shown. The flux collector is connected to a MHV feedthrough via a shielded cable. A shutter at the output of the source may be actuated by a small rotary feedthrough.

IV. OPERATION AND EXAMPLES

In its mode as a molecular beam epitaxy source, the operation of the present IBAD–MBE source is similar to that of the commercial EFM3 source.[25] However, since for IBAD applications a high proportion of self-ions at the target is desired, the region around the evaporator tip and the filament has been redesigned to maximize the production and extraction efficiency of ions. This was done by means of ion and electron trajectory calculations using SIMION.[33] While the design goal was achieved satisfactorily, it also turned out that the position of filament and evaporator tip inside the enclosure is more critical than in the previous design. Since a visual inspection of the tip position was considered impractical, a procedure based on electrical measurements was developed to find the proper tip position. The suggested procedure is the following: Initially, the evaporator rod is pushed forward well beyond the plane of the circular filament. The filament is heated by a constant current (around 2 A) and one waits until a constant emission current of 5–10 mA at about +700 V at the rod is reached. In order to prevent thermal electrons to reach the lens and flux electrodes, a constant bias potential of +5 V with respect to the grounded enclosure is always applied to the filament. At these conditions little or no evaporation occurs (with a Ni rod in this case) and the cylindrical diode formed of rod and filament is in its saturated mode. Then the rod is slowly retracted while the emission current is observed. Initially, the emission stays constant, but starts to drop slowly when the rod is retracted beyond the filament plane. The proper setting of the evaporator tip is reached, if the emission current has dropped to 75%–80% of its constant initial value. At this position the flux of ions and neutrals at the target reaches a saddle point (lens and flux electrode grounded). Retracting the rod further increases both fluxes, but in the constant emission current mode used in actual operation the heating power to the filament increases steeply, thus shortening the filament lifetime. Alternatively, one may stabilize the emission current at a higher level (e.g., 10 mA) and increase the rod voltage, until evaporation starts and a useful ion current develops (e.g., 900 V for Ni). This ion current may be measured by connecting the lens and flux electrode together, thus forming essentially a Faraday cup for the ions leaving the orifice in the top plate of the Cu housing. Moving the rod slightly back and forth one then observes a shallow maximum of the total ion current,

TABLE I. Typical operation conditions of the source in the MBE mode with Ni as an example. The working distance from the end of source to target was 51 mm. The optimum rod position had been adjusted according to the two independent procedures. The lens electrode is grounded. Therefore, the metal ions are not focussed and the ion fraction is very small.

Material	Ni
Emission current	10 mA, stabilized
High voltage at rod	950 V
Total target ion-current	2.8 nA
Ion flux density	1.7×10^{10} ions/cm^2 s
Flux collector current	67 nA
Deposition rate	1.6 Å/min (quartz monitor)
Ion fraction	6.9×10^{-4} ions/atom

centered around the position determined previously. The maximum of the ion current means that at the proper tip position of the rod a relative maximum of the total ion flux in the forward direction through the orifice is obtained. The proper position of the rod may thus be determined in two independent ways, yielding the same optimum position within ±0.3 mm. Once this position is found, the shortening of the rod due to evaporation may be compensated by using the linear motion feedthrough. Since at constant emission current the heating power to the filament increases upon recession of the tip, it suffices to push the rod forward until the previous heating current (or, more sensitively, the filament voltage) is restored. A heating current and/or voltage monitor with 3 1/2 digits resolution is recommended.

With the optimum position found, the source may be used in the MBE mode in the usual way: The focusing lens is grounded and the current to the flux electrode is used to monitor the vapor flux. The latter may then be calibrated against a quartz oscillator[34] at the target position or by observing diffracted intensity oscillations in layer-by-layer growth of a film. Typical operating parameters for Ni deposition at a working distance of 51 mm from end of source to target are given in Table I. The ion fraction is obtained from the ratio of target current to deposition rate, assuming only singly charged ions. The neutral and ion flux spatial distribution can safely be assumed to be the same since no electrical potentials act on the ions once they passed the orifice, i.e., both fluxes come approximately from the same source area and are confined by the same opening at the end of the source.

A. Mode 1: Metal deposition without ions

The ion fraction of less than 10^{-3} is likely not to cause significant additional defects beyond those left by the deposition process in most cases. However, for very sensitive materials or very high ionization probability one may wish to suppress all ions. In the present design this can easily be done by raising the lens potential to the rod potential. We did this and observed a complete suppression of the ion current. The disadvantage is that the continuous monitoring of the deposition rate is lost. Alternatively, one may apply a positive potential to the flux electrode. By suitable adjustment of this potential one may block the ions to reach the target and simultaneously reflect a large part of the ion flux onto the lens electrode, where it can be measured together with the ions reaching the lens electrode. (We measured these currents to be similar when both electrodes are close to ground.) This mode of operation requires a recalibration of ion current verous deposition rate, but maintains two useful features of the source: (i) by integrating the ion current one has a very convenient means of determining the film thickness at every instance and (ii) the ion current may be fed back to the HV power supply for the evaporation rod to maintain constant deposition rate by altering the heating power to the rod (the change of ionization cross section with electron energy is negligible for small voltage changes). On the other hand, in this mode of ion suppression the flux electrode couples capacitively into the lens electrode, causing displacement currents. Therefore, a very stable and noise-free power supply is required. The arrival of negative ions at the target was never observed.

TABLE II. Typical operating conditions of the source in the mode metal-ion beam assisted deposition of Co onto Cu(111). The flux electrode is grounded. Potentials are given with respect to ground. The ion energy is close to the high-voltage at the rod (see Fig. 1).

Material	Co
Emission current	14 mA, stabilized
High voltage at rod	+600 V
Lens voltage	+470 V
Total target current	32 nA
Ion flux density at target, average across 5 mm ϕ	7×10^{11} ions/cm^2 s
Deposition rate	0.4 ML/min
Ion fraction	5.9×10^{-2} ions/atom

B. Mode 2: Ion beam assisted deposition using metal ions

Ion beam assisted deposition using ions from the vapor itself has the great advantage of not introducing any foreign material into the film. The crucial parameter in this mode is the fraction of ions arriving per vapor atom. The energy of the ions is also of importance since high energy ions create more adatoms than low energy ones,[23] thus enhancing the nucleation density, but they also penetrate deeper into the film and substrate, causing defects that are more difficult to remove. In addition, the decrease of the island number density by athermal effects caused by the collision cascade is smaller for low energies than for higher ones.[24] Therefore, we focused our attention to low ion energies ($\sim$600 eV). When reducing the voltage at the evaporation rod the heating power drops, which can be compensated by increasing the emission current. This has the additional benefit of increasing the ionization rate by electron impact on to the vapor atoms. The ions leaving the aperture in the grounded top plate of the Cu housing are focused onto the target by applying a voltage of 75%–80% of the evaporator rod potential (depending upon the working distance). The optimum focusing condition is indicated by a maximum of the target current coinciding with a clear minimum of the current to the flux electrode. At a working distance of 51 mm the ion beam spot size at the target is about 5 mm in diameter full width at half maximum. The typical operating conditions for Co on Cu(111) are given in Table II. The ion flux density onto a 5 mm diam spot on the sample increases by a factor of 50–60

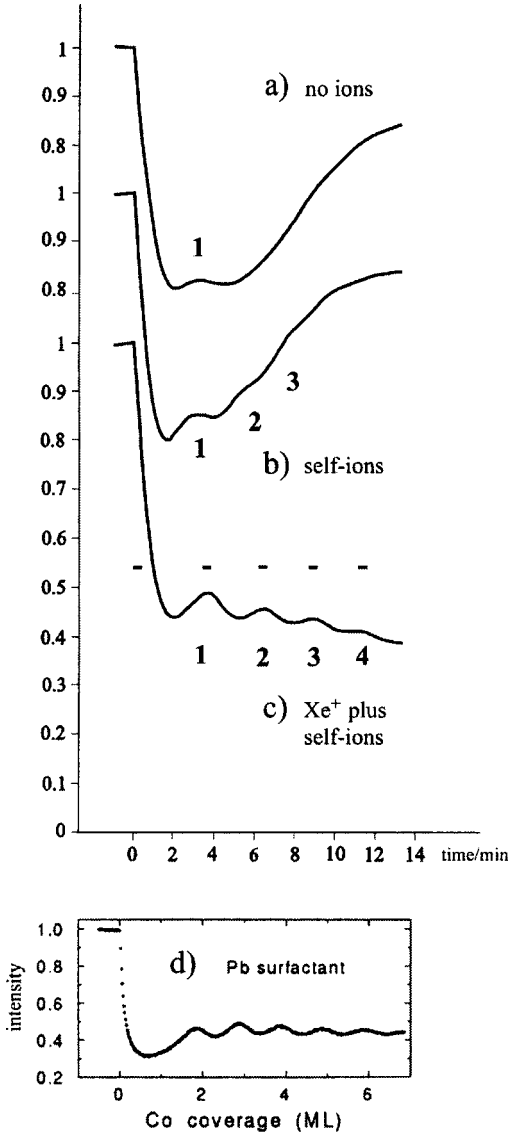

FIG. 4. Results for Co-deposition onto Cu(111) are given in panels (a)–(c). Shown is the intensity of the (00) beam as a function of time after opening the shutter. The sample temperature is 80 °C in all cases. (a) Operation of the source in the MBE mode. There is only one minor maximum visible. This result is typical for three-dimensional growth. (b) Operation in the ion beam assisted deposition mode using self-ions. (cf. Table II) A number of oscillations are visible on a rising background, indicating an intermediate stage between three-dimensional growth and layer-by-layer growth. (c) operation in the pulsed IBAD mode with Xe gas added. See Table III for the parameters. The ion beam is switched on for 25 s at the beginning and near each maximum, indicated by the short horizontal bars. A good layer-by-layer growth is achieved. For comparison panel (d) shows a result from the literature (see Ref. 11) for the same system using Pb as a surfactant.

compared to the lens at ground. In our actual example, this results in an ion fraction of about 6%. The determination of the deposition rate has been made by observing the intensity oscillations of a diffracted electron beam as explained later.

C. Mode 3: Ion beam assisted deposition with pulsed ion beam

Ion beam assisted deposition with self-ions in the pulsed mode may be easily performed with our source by switching the lens potential from the potential of the evaporation rod (suppression of ions) to the optimum focusing voltage in a pulsed mode. However, with our combination of film and substrate this resulted only in a marginal improvement of the growth mode beyond the very significant improvement achieved by IBAD in the continuous mode [see Fig. 4(b)]. This should not be taken as a general rule, but may depend strongly on the material and substrate.[20–24]

TABLE III. Parameters for ion beam assisted deposition using the additional gas inlet with Xe. The system is pumped by a turbomolecular pump with a Ti sublimator. The effective pumping speed at the target location was 40 l/s for Xe.

Material	Co
Emission current	14 mA, stabilized
High voltage at rod	+600 V
Lens voltage	+470 V
Growth rate	0.4 ML/min
Total target current	70 nA
Ion flux density	1.5×10^{12} ions/cm^2 s
Xe gas flux	8.5×10^{-6} mbar l/s
Pressure at target (ion gange corrected for Xe)	2×10^{-7} mbar
Ion fraction	1.27×10^{-1} ions/atom

D. Mode 4: Ion beam assisted deposition with rare gas ions

Our IBAD–MBE source provides additional flexibility by admitting gas into the ionization region through a capillary aiming at the tip of the evaporation rod. We had mainly noble gases in mind, but reactive gases such as O_2 or N_2 may also be used, e.g., when oxide or nitride layers are desired. An improvement of the oxidation by molecular or atomic ions may be expected, reaching into depth by virtue of the kinetic energy of the ions. In our example, we used Xe, since due to its low ionization potential ions are created efficiently. Generating ions independently of the metal evaporation allows for greater flexibility in the choice of ion energy and deposition rate. The operation of the source in this mode is simple, requiring little more than an additional leak valve and gas bottle. Our system was pumped by a 180 l/s turbo molecular pump, yielding an effective pumping speed of 40 l/s for Xe (110 l/s for N_2) at the location of the target. Typical operating conditions are shown in Table III. An ion fraction of about 10% is easily obtained at a moderate gas throughput of less than 10^{-5} mbar l/s. The focusing conditions as well as the operation in the pulsed mode (mode 5) are the same as described in the previous section. As shown in the next paragraph, a very substantial improvement of the growth mode may be achieved in the pulsed mode.

V. EXAMPLE: DEPOSITION OF Co ON Cu(111)

The system Co on Cu(111) is notorious for its poor layer-by-layer growth. Its tendency to grow in three-dimensional islands from the very beginning has previously been overcome in two ways: (i) pulsed laser MBE or (ii) addition of a surfactant. Due to the high nucleation rate in laser MBE, good layer-by-layer growth and the suppression of stacking faults have been demonstrated.[35–38] The addition of 1.5 ML of lead as a surfactant and a careful heat treatment have been shown to produce good films by lowering the Ehrlich–Schwoebel barrier.[11,12] However, the first alternative

is rather involved and expensive. The second alternative is relatively convenient, but leaves a layer of Pb on the surface which may be undesirable.

In the following we show in three examples how our IBAD–MBE source performs on this system.

In all cases, the growth behavior was controlled by medium energy electron diffraction. An electron beam of 2–3 keV energy impinges at a grazing angle of 3°–5° onto the Cu(111) crystal. The elastically diffracted beams are observed on a low—energy electron diffraction (LEED) screen which is mounted opposite to an Auger analyzer, whose electron gun is used as the source of electrons. Usually, the intensity of the (00) beam is monitored by a spot photometer. By varying the primary beam energy and the angle of incidence a relative maximum of the diffracted intensity is sought. According to (our) experience this insures that peaks in diffracted intensity during layer-by-layer growth coincide closely with filled layer coverage, while the minima correspond to half filled layers. The IBAD–MBE source is mounted perpendicular to the axis of the electron beam, which results in nearly perpendicular incidence of the vapor and ion fluxes. The Auger analyzer and the LEED system are used to monitor the cleanliness and structure of substrate and film. The sample temperature was kept constant at $80\pm3\,^{\circ}\mathrm{C}$ by radiative heating of the crystal and cooling with liquid nitrogen. The deposition rate was determined by the quartz crystal oscillator[34] mounted beneath the sample, which could be moved in the crystal position by a vertical displacement of the sample manipulator. The ion beam profile was measured by a horizontal edge below the deposition monitor. In the growth experiments, the diffracted intensity of the (00) beam was measured as a function of time elapsed after the opening of the shutter, see Fig. 4.

First, we operated our source in the MBE mode with or without ion suppression. The result is shown in Fig. 4(a). After an initial steep drop a weak maximum develops, followed by a subsequent rise to about 80% of the initial intensity. No further intensity oscillations are seen and the growth is clearly not layer-by-layer. From previous scanning tunneling microscopy studies[36] we know that large three-dimensional pyramids of triangular shape develop. We found no difference in the growth behavior when the residual ion current was turned on or off by the lens potential.

Next we operated the source in the continuous IBAD mode with metal ions. The operating parameters are given in Table II and the result is shown in Fig. 4(b). The first maximum is more pronounced and two more maxima are visible. This indicates that a self-ion fraction of about 6% may lead to a substantially improved layer-by-layer growth. Operating the source in the pulsed mode with a pulse length of 30 s did not result in a substantial improvement. Though a good layer growth was not yet achieved, the number of oscillations is sufficient to determine the growth rate (0.4 ML per minute). This agreed well with the deposition rate determined by the quartz crystal oscillator. The same deposition parameters of the source were used for all three measurements(a)–(c) in Fig. 4. A readjustment of the evaporation rod position according to the procedure described in Sec. IV was made in between to test the reproducibility of the deposition rate. Routinely, a margin of 10% is obtained, which can be improved to less than 5% by carefully adjusting the critical parameters (mainly high voltage on the evaporation rod, emission current, and heating current and voltage at the filament).

A very substantial improvement of the growth mode is achieved in the pulsed IBAD mode with additional Xe^+ ions, see Fig. 4(c). Before opening the shutter, the evaporation conditions were set with the lens at ground potential, monitoring the current to the flux electrode. The same settings as for IBAD with self-ions were used. Then Xe gas was let in until the flux electrode current increased by a factor of 2. A preliminary estimate indicates that the ion current density at the target should then also double (in fact it was slightly higher, compare Tables II and III).

Then the lens potential was adjusted for focusing and the shutter was opened. The diffracted intensity dropped rapidly until half its initial value, when the lens was switched to ground potential. This ion pulse serves to create a number of nucleation sites at adatoms, mainly Cu atoms ejected from the substrate. Then the growth of the first layer proceeds, indicated by a minimum followed by a subsequent rise of the intensity. Shortly before the maximum is reached, the lens is turned on for 25 s, which provides a pulse of $3.8\times10^{13}\,\mathrm{ions/cm^2}$. These ions create new nucleation centers on top of the almost completed first layer which serve to stimulate the growth of the second layer in a smooth way. The duration of the ion pulse is indicated by small horizontal bars in Fig. 4(c). This procedure is repeated each time when a relative intensity maximum approaches and a good layer-by-layer growth up to 4 1/2 layers is achieved in this case. More details on the growth scenario with pulsed IBAD are given in Refs. 21 and 22. For comparison we show a result from the literature[11] for the same system using Pb as a surfactant [Fig. 4(d)]. The comparison shows, that a quite satisfactory layer-by-layer growth may be achieved by our IBAD–MBE source in the pulsed mode. In the continuous mode the results were not better than for metal-ions only [see Fig. 4(b)].

When one compares the ion flux densities in Tables II and III one finds that the ion beam in the IBAD mode with additional Xe gas is composed of Co^+ and Xe^+ ions in about equal proportions. One may wonder why a factor of 2 in ion flux density may lead to such a drastic improvement in the growth mode. This may be attributed to the fact that the efficiency of adatom creation is much higher for Xe than for Co (and Ni) because of its higher mass. We found evidence for this by observing the initial drop of intensity after opening the shutter. With self-ions plus Xe ions the initial decrease is indeed much stronger than one finds for metal-ions alone. Our observations confirm with a ''difficult'' materials system the dramatic improvement of layer growth by pulsed ion beam assisted deposition and demonstrate the usefulness of our IBAD–MBE source.

The present results have been obtained by relatively unsophisticated experimental means: a spot photometer, a strip-chart recorder, visual inspection, and manual switching. An improved version would utilize a computer, a TV camera with frame grabber, and an adaptive program using a predictor-corrector scheme. One would observe a number of

diffracted electron beams simultaneously plus the diffuse background to obtain a more complete picture of the growing layer and the defect density. A particular problem is the proper on and off times of the ion beam, associated with the completion of a monolayer. By visual inspection one has to guess the time at which the next maximum of diffracted intensity may occur. This becomes difficult when the amplitude of the oscillations slowly decreases with increasing layer thickness. An adaptive computer program would determine the oscillation period from a multitude of diffracted beams for the first two oscillations and then use an adaptive extrapolation routine to determine the start and duration of the next ion pulse, actuated by the computer. In this way small drifts of the deposition rate could also be compensated. Using such devices in combination with our IBAD–MBE source may greatly improve the capabilities of growing epitaxial thin films.

ACKNOWLEDGMENTS

Enlightening discussions with W. Wulfhekel on ion beam enhanced growth processes are gratefully acknowledged. The authors also thank W. Eberhardt, K. Haenecke, and M. Oppelt for their expert help during the early stages of the project.

[1] F. A. Smidt, Int. Mater. Rev. **35**, 61 (1990).
[2] J. K. Hirvonen, Mater. Sci. Rep. **6**, 215 (1991).
[3] W. Ensinger, Rev. Sci. Instrum. **63**, 5217 (1992).
[4] F. A. Smidt and G. K. Hubler, Nucl. Instrum. Methods Phys. Res. B **880/81**, 207 (1993).
[5] S. Mohan and M. Ghanashyam Krishna, Vacuum **46**, 645 (1995).
[6] M. Copel, M. C. Reuter, E. Kaxiras, and R. M. Tromp, Phys. Rev. Lett. **63**, 632 (1989); Appl. Surf. Sci. **91**, 182 (1995).
[7] E. Tournie and K. H. Ploog, Thin Solid Films **231**, 43 (1993).
[8] S. Esch, M. Hohage, T. Michely, and G. Comsa, Phys. Rev. Lett. **72**, 518 (1994).
[9] W. F. Egelhoff, Jr. *et al.*, J. Appl. Phys. **80**, 5183 (1996).
[10] I. Markov, Mater. Chem. Phys. **49**, 93 (1997); Surf. Sci. **429**, 102 (1999).
[11] J. Camarero *et al.*, Phys. Rev. Lett. **76**, 4428 (1996).
[12] J. E. Prieto, Ch. Rath, K. Heinz, and R. Miranda, Surf. Sci. **454–456**, 736 (2000).
[13] G. Rosenfeld, R. Servaty, C. Teichert, B. Poelsema, and G. Comsa, Phys. Rev. Lett. **71**, 895 (1993).
[14] V. S. Stepanyuk, D. I. Bazhanov, A. N. Baranov, W. Hergert, A. A. Katsnelson, P. H. Dederichs, and J. Kirschner, Appl. Phys. A: Mater. Sci. Process. **A72**, 443 (2001).
[15] V. S. Stepanyuk, D. I. Bazhanov, W. Hergert, and J. Kirschner, Phys. Rev. B **63**, 153406 (2001).
[16] K. L. Saenger, Process. Adv. Materials **3**, 1 (1993); **3**, 63 (1993).
[17] H. U. Krebs, Int. J. Non-Equilib. Process. **10**, 3 (1997).
[18] H. Jenniches, M. Klaua, H. Hoeche, and J. Kirschner, Appl. Phys. Lett. **69**, 3339 (1996).
[19] G. Rosenfeld, N. N. Lipkin, W. Wulfhekel, J. Kliewer, K. Morgenstern, B. Poelsema, and G. Comsa, Appl. Phys. A: Mater. Sci. Process. **61**, 455 (1995).
[20] W. Wulfhekel, N. N. Lipkin, J. Kliewer, G. Rosenfeld, L. C. Jorritsma, B. Poelsema, and G. Comsa, Surf. Sci. **348**, 227 (1996).
[21] W. Wulfhekel, I. Beckmann, N. N. Lipkin, G. Rosenfeld, B. Poelsema, and G. Comsa, Appl. Phys. Lett. **69**, 3492 (1996).
[22] W. Wulfhekel, I. Beckmann, G. Rosenfeld, B. Poelsema, and G. Comsa, Surf. Sci. **395**, 168 (1998).
[23] M. Morgenstern, T. Michely, and G. Comsa, Philos. Mag. A **79**, 775 (1999).
[24] S. Esch, M. Breeman, M. Morgenstern, T. Michely, and G. Comsa, Surf. Sci. **365**, 187 (1996).
[25] An improved version of the original design is available from Omicron Inc., type EFM3.
[26] T. Jones, J. Sawler, and D. Venus, Rev. Sci. Instrum. **64**, 2008 (1993).
[27] B. T. Jonker, J. Vac. Sci. Technol. A **8**, 3883 (1990).
[28] Kimball Physics Inc., type MCF 275-FM1R05-A.
[29] Ceramaseal Inc., type 10185-O2-CF.
[30] Eheim GmbH, Plochingerstr. 54, 72779 Deizisau, Germany, type 1250219, universal pump.
[31] Huntington Mechanical Laboratories Inc., type VF-178-133.
[32] Dunyway Stockroom Corp., type VLVE-2000.
[33] Princeton Electronic Systems Inc., SIMION 3 D, version 6.0 by David A. Dahl.
[34] Inficon Inc., type Deposition Controller XTC/2.
[35] M. Zheng, J. Shen, C. V. Mohan, P. Ohresser, J. Barthel, and J. Kirschner, Appl. Phys. Lett. **74**, 425 (1999).
[36] M. Zheng, J. Shen, J. Barthel, P. Ohresser, C. V. Mohan, and J. Kirschner, J. Phys.: Condens. Matter **12**, 783 (2000).
[37] J. Shen, P. Ohresser, C. V. Mohan, M. Klaua, J. Barthel, and J. Kirschner, Phys. Rev. Lett. **80**, 1980 (1998).
[38] P. Ohresser, J. Shen, J. Barthel, M. Zheng, C. V. Mohan, M. Klaua, and J. Kirschner, Phys. Rev. B **59**, 3696 (1999).